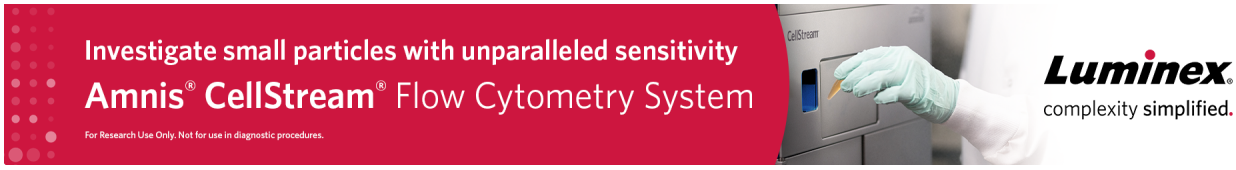

The Journal of Immunology

Allergic Airways Disease Develops after an Increase in Allergen Capture and Processing in the Airway Mucosa

Christophe von Garnier, Matthew E. Wikstrom, Graeme Zosky, Debra J. Turner, Peter D. Sly, Miranda Smith, Jennifer A. Thomas, Samantha R. Judd, Deborah H. Strickland, Patrick G. Holt and Philip A. Stumbles

J Immunol 2007; 179:5748-5759; ;
doi: 10.4049/jimmunol.179.9.5748
http://www.jimmunol.org/content/179/9/5748

This information is current as of October 27, 2021.

References This article **cites 46 articles**, 20 of which you can access for free at:
http://www.jimmunol.org/content/179/9/5748.full#ref-list-1

Why *The JI*? Submit online.

- **Rapid Reviews! 30 days*** from submission to initial decision
- **No Triage!** Every submission reviewed by practicing scientists
- **Fast Publication!** 4 weeks from acceptance to publication

**average*

Subscription Information about subscribing to *The Journal of Immunology* is online at:
http://jimmunol.org/subscription

Permissions Submit copyright permission requests at:
http://www.aai.org/About/Publications/JI/copyright.html

Email Alerts Receive free email-alerts when new articles cite this article. Sign up at:
http://jimmunol.org/alerts

The Journal of Immunology is published twice each month by
The American Association of Immunologists, Inc.,
1451 Rockville Pike, Suite 650, Rockville, MD 20852
Copyright © 2007 by The American Association of Immunologists All rights reserved.
Print ISSN: 0022-1767 Online ISSN: 1550-6606.

Downloaded from http://www.jimmunol.org/ by guest on October 27, 2021

Allergic Airways Disease Develops after an Increase in Allergen Capture and Processing in the Airway Mucosa[1]

Christophe von Garnier,[2,3]* Matthew E. Wikstrom,[2]* Graeme Zosky,* Debra J. Turner,* Peter D. Sly,* Miranda Smith,* Jennifer A. Thomas,* Samantha R. Judd,* Deborah H. Strickland,* Patrick G. Holt,* and Philip A. Stumbles[3]*†

Airway mucosal dendritic cells (AMDC) and other airway APCs continuously sample inhaled Ags and regulate the nature of any resulting T cell-mediated immune response. Although immunity develops to harmful pathogens, tolerance arises to nonpathogenic Ags in healthy individuals. This homeostasis is thought to be disrupted in allergic respiratory disorders such as allergic asthma, such that a potentially damaging Th2-biased, $CD4^+$ T cell-mediated inflammatory response develops against intrinsically nonpathogenic allergens. Using a mouse model of experimental allergic airways disease (EAAD), we have investigated the functional changes occurring in AMDC and other airway APC populations during disease onset. Onset of EAAD was characterized by early and transient activation of airway $CD4^+$ T cells coinciding with up-regulation of CD40 expression exclusively on $CD11b^-$ AMDC. Concurrent enhanced allergen uptake and processing occurred within all airway APC populations, including B cells, macrophages, and both $CD11b^+$ and $CD11b^-$ AMDC subsets. Immune serum transfer into naive animals recapitulated the enhanced allergen uptake observed in airway APC populations and mediated activation of naive allergen-specific, airway $CD4^+$ T cells following inhaled allergen challenge. These data suggest that the onset of EAAD is initiated by enhanced allergen capture and processing by a number of airway APC populations and that allergen-specific Igs play a role in the conversion of normally quiescent AMDC subsets into those capable of inducing airway $CD4^+$ T cell activation. ***The Journal of Immunology,*** **2007, 179: 5748–5759.**

The respiratory tract (RT)[4] is continuously exposed to environmental Ags ranging from innocuous substances to potentially harmful pathogens. Discrimination of harmless and harmful airborne Ags at this site therefore represents a constant challenge to the local airway mucosal immune system. In healthy individuals, nonreactivity or tolerance to inhaled innocuous foreign Ags normally arises as a default response to repeated exposure (1, 2). This immunological homeostasis, however, may be disrupted following infection or in atopic disorders, such as allergic asthma, generating an inappropriate and potentially tissue-damaging response to seemingly nonpathogenic allergens (3, 4). Although recent research activity has centered on the dendritic cell (DC):T cell interaction and downstream events during allergic sensitization of RT, most studies have focused on lung tissue, rather than on the conducting airways where airways hyperresponsiveness (AHR) is initiated. Furthermore, there is incomplete knowledge about the kinetics and functional changes occurring in other airway APC populations. We and other investigators have recently shown the complexity of different APC populations within the RT, with B cells, macrophages, DC precursors, and DC subsets potentially capable to interact and influence the outcome of sensitization (5, 6).

An essential function of RT-APC, and RT-DC in particular, is the uptake and processing of inhaled Ags and pathogens in a format suitable for surveillance by recirculating $CD4^+$ T cells. We have previously hypothesized this is a continuous sampling process that under normal, noninflammatory circumstances is tightly regulated such that a functional T cell signal will only be provided once the RT-DC has left the tissue microenvironment and migrated to the draining lymph nodes (DLN) (7, 8). We and others have argued that this is necessary to avoid local activation of T cells within the airway mucosa and the potentially damaging inflammation that would ensue (4, 8).

In the current study, we have tested the hypothesis that disruption of the normally tightly regulated RT-DC Ag-uptake and -processing function is integrally associated with the early induction phase of T cell-mediated allergic AHR. Using a mouse model of allergic airways inflammation, our data indicate that the onset of the characteristic clinical features of AHR, including physiological changes, Ig production (both IgG and IgE), and inflammatory cell influx, is closely linked to a transient increase in activated $CD4^+$ T cells within the airways and is preceded by up-regulation in the capacity of several airway APC populations to capture and degrade

*Telethon Institute for Child Health Research and Centre for Child Health Research, School of Pediatrics and Child Health, University of Western Australia, West Perth, Western Australia, Australia; and †School of Veterinary and Biomedical Sciences, Division of Health Sciences, Murdoch University, Perth, Western Australia, Australia

Received for publication March 30, 2007. Accepted for publication August 17, 2007.

The costs of publication of this article were defrayed in part by the payment of page charges. This article must therefore be hereby marked *advertisement* in accordance with 18 U.S.C. Section 1734 solely to indicate this fact.

[1] This work was supported by National Health and Medical Research Council of Australia. C.v.G. was funded by the Swiss National Fund, Janggen-Poehn-Stiftung, Herrmann-Stiftung, Novartis-Stiftung, and Boehringer Ingelheim.

[2] C.v.G. and M.E.W. have contributed equally to this work.

[3] Address correspondence and reprint requests to Dr. Christophe von Garnier at the current address: Respiratory Medicine, Berne University Hospital, 3010 Berne, Switzerland; E-mail address: christophe.vongarnier@insel.ch or Dr. Philip A. Stumbles, Division of Cell Biology, Telethon Institute for Child Health Research, P.O. Box 855, West Perth, Western Australia 6872, Australia; E-mail address: phils@ichr.uwa.edu.au

[4] Abbreviations used in this paper: RT, respiratory tract; DC, dendritic cell; AHR, airway hyperresponsiveness; DLN, draining lymph node; EEAD, experimental allergic airways disease; BLG, β-lactoglobulin A; p.n., per nasal; MCh, methacholine; BAL, bronchoalveolar lavage; Alum, $AlOH_3$; MHC II, MHC class II.

Copyright © 2007 by The American Association of Immunologists, Inc. 0022-1767/07/$2.00

Downloaded from http://www.jimmunol.org/ by guest on October 27, 2021

inhaled protein allergen. In particular, we suggest that local $CD4^+$ T cell activation is likely to be driven in this model by a population of $CD11b^-$ airway mucosal DC that uniquely express the costimulatory molecule CD40 during the early stages of disease onset. Furthermore, we also present data supporting the conclusion that the enhanced allergen uptake and processing capacity of APC within the airway mucosa is mediated by allergen-specific Igs that aid Ag capture by airway APC populations. These data highlight the need the need for multiple target strategies in the treatment and prevention of allergic AHR, including interventions that target DC-, T cell-, and Ab-driven pathogenic processes.

Materials and Methods

BALB/c mouse model of experimental allergic airways disease (EAAD)

BALB/c mice were bred specific pathogen free at the Animal Resource Centre (Perth, Australia) and housed under clean conditions on low-dust bedding at the Telethon Institute for Child Health Research (TICHR). BALB/c DO11.10 TCR-transgenic mice recognizing an $I\text{-}A^d$-restricted epitope of OVA ($OVA_{323–339}$; peptide sequence ISQAVHAAHAEI NEAGR) were purchased from The Jackson Laboratory and maintained under clean conditions. All mice were used as females of 8–10 wk of age and given free access to feed and water. As shown in Fig. 1*A*, mice were sensitized by i.p. injection with 20 μg of OVA (Sigma-Aldrich) suspended in 200 μl (4 mg) of $AlOH_3$ (Alum; Alu-gel-S; Serva) on days 0 and 14. Mice were then challenged with either one or three OVA (1% w/v in PBS) aerosols delivered with an ultrasonic nebulizer (DeVilbiss UltraNeb) for 30 min on consecutive days starting at day 21. Additional groups of mice served as controls: a naive group and a group that received i.p. PBS and was challenged with OVA aerosols using the protocol described above. In other experiments, mice were sensitized by i.p. injection with 10 μg of β-lactoglobulin A (BLG) from bovine milk (Sigma-Aldrich) suspended in 200 μl of Alum (Alu-gel-S; Serva) on days 0 and 14. Animal experiments were approved by the TICHR Animal Experimentation Ethics Committee operating under guidelines in accordance with the Australian Code of Practice for the Care and Use of Animals for Scientific Purposes.

Cell preparations from lung and conducting airways

Animals were euthanized by i.p. injection of 100 μl of phenobarbitone sodium (Lethabarb; Virbac). Lung and heart were exposed by bilateral thoracotomy and the aorta and inferior vena cava were cut to exsanguinate animals before perfusion of the right ventricle with at least 5 ml of PBS. Thereafter, the peripheral third of the lung was excised (further referred to as lung parenchyma) and airways, including the trachea and the main bronchi (further referred to as main conducting airways), were prepared. Lung parenchyma was chopped into 2-mm slices using a McIlwain tissue chopper (Mickle Laboratory Engineering) and main conducting airways were manually sliced into thin pieces. Cell isolation procedures were conducted in a solution of 11 mM D-glucose, 5.5 mM KCl, 137 mM NaCl, 25 mM Na_2HPO_4, and 5.5 mM $NaH_2PO_4 \cdot 2\ H_2O$ (GKN) supplemented with 10% FCS as indicated. Tissue was transferred into 30 ml of GKN-10% FCS containing 1.8 mg/ml collagenase type 4 (Worthington Biochemical) and 0.1 mg/ml DNase I (Sigma-Aldrich) and incubated for 90 min at 37°C in a shaking water bath. After 60 min, an additional 0.1 mg/ml DNase I was added to the tracheal digests. Unless indicated otherwise, all subsequent procedures were strictly performed on ice. Tissue was disrupted with a plastic transfer pipette until most of the larger tissue pieces were dispersed. The digest mixture was then passed through a cotton wool filter to remove tissue debris. After one wash in GKN-10% FCS, RBC lysis was performed with NH_4Cl and cells were resuspended in fluorescence buffer (PBS containing 0.5% BSA and 0.1% sodium azide) after one wash.

Flow cytometry

All Abs were obtained from BD Pharmingen, unless indicated otherwise. All incubations were performed on ice throughout the procedure and included an Fc block (anti-mouse CD16/CD32) added for 10 min to reduce nonspecific binding. T cells were identified using a combination of Abs against CD3 and CD4, and early activation was measured with an Ab against CD69. APCs were identified using Abs against CD11c, I-A/E (MHC class II), and CD11b, as described previously, and activation was assessed with Abs against CD40, CD80, and CD86 (5). OVA-specific $CD4^+$ T cells were identified in DO11.10 mice using the KJ1–26 mAb (Caltag Laboratories) and naive cells were distinguished from memory cells on the basis of CD44 expression, where naive T cells are $CD44^{low}$. Relevant isotype control Abs were used throughout to differentiate specific binding from nonspecific binding or background fluorescence. Cell samples were collected using a four-color FACSCalibur or a six-color LSRII (BD Biosciences) and analyzed with FlowJo Software (Tree Star).

Ag-tracking studies

Ag uptake and processing was tracked in vivo by administering a variety of fluorescent conjugates, as described previously (9). OVA-Alexa Fluor 647 (Molecular Probes) was used to track OVA uptake; an Alexa Fluor 647 conjugate of BLG was prepared using a protein labeling kit (Molecular Probes) according to the manufacturer's instructions. DQ-OVA (Molecular Probes) was used to track OVA processing. A total of 20–50 μg of each conjugate was administered per nasal (p.n.) in a 50-μl volume by gradual application to the nares during halothane or isoflurane anesthesia. Two hours later, the main conducting airways were collected and prepared for flow cytometry as described above. Ag uptake and processing was assessed in various cell types by comparison with a group of mice administered 50 μl of saline p.n. (saline control).

Measurement of AHR

AHR to inhaled methacholine (MCh) was measured using a modification of the low-frequency forced oscillation technique as previously described (10). Briefly, mice were anesthetized, tracheostomized and ventilated using a custom built ventilator (flexiVent; Scireq) that functioned both as a ventilator and means of measuring respiratory system input impedance (Zrs). Zrs was measured during periods of apnea by applying a 16-s signal containing 19 mutually prime sinusoidal frequencies ranging from 0.25 to 19.625 Hz. The real and imaginary parts of the Zrs spectrum were fit to the constant-phase model allowing calculation of changes in airway resistance (raw), tissue damping (G), tissue elastance (H) (11). The changes in these parameters were measured in response to 90-s MCh aerosols generated using an ultrasonic nebulizer (UltraNeb; DeVilbiss) ranging in dose from 0.1 to 30 mg/ml.

Specific Ab determination by time-resolved fluorescence assay

Sera were analyzed for the presence of total IgE and OVA-specific IgG2a and IgG1 Abs by time-resolved fluorescence assays. Briefly, 96-well plates (Nunc Maxisorp) were coated overnight at 4°C with 10 μg/ml OVA for determination of OVA-specific IgG1, or with anti-mouse IgE (R35-72; BD Pharmingen) for total IgE measurements. Plates were blocked with 200 μl of 0.5% BSA in Tris-HCl (pH7.4) for 1 h at room temperature on a plate shaker. For all subsequent steps, a volume of 50 μl/well was used and incubations were performed during 1 h at room temperature unless otherwise indicated. Between steps, plates were washed five times with wash buffer Tris-HCl (pH 7.8) Tween 20. As interassay standards, mouse anti-OVA IgG1 (Hyb 099-09) and monoclonal mouse IgE (BD Pharmingen) were used. Sera were diluted 1/10 in Delfia assay buffer (Wallac Oy). Biotinylated anti-mouse IgE (R35-118) and IgG1 (A85-1; The Antibody Shop) were purchased from BD Pharmingen and used at 2 μg/ml. Streptavidin-conjugated europium (Wallac Oy) was incubated at 1/500 for 30 min and plates were washed eight times thereafter. Delfia enhancement solution (Wallac Oy) was added and plates were agitated on a shaker during 10 min before reading the fluorescence on a Wallac Victor 2 counter (Wallac Oy).

Bronchoalveolar lavage (BAL) fluid inflammatory cell counts

Separate groups of sensitized and control mice were euthanized and tracheostomized to collect BAL fluid. The BAL fluid was centrifuged at 2000 rpm for 4 min. Following the removal of the supernatant, the pellet was resuspended in PBS and cells were stained with trypan blue to determine the total cell count and live cell count (trypan blue exclusion). Differential counts were obtained from the cytospin sample, stained with Diffquick stain (LabAids), and examined using light microscopy and counting at least 300 cells.

Passive immunization

OVA-immune serum was collected from OVA-sensitized BALB/c mice 48–72 h after they had been challenged with three OVA aerosols, as described above. Control serum was collected at the same time from BALB/c

Downloaded from http://www.jimmunol.org/ by guest on October 27, 2021

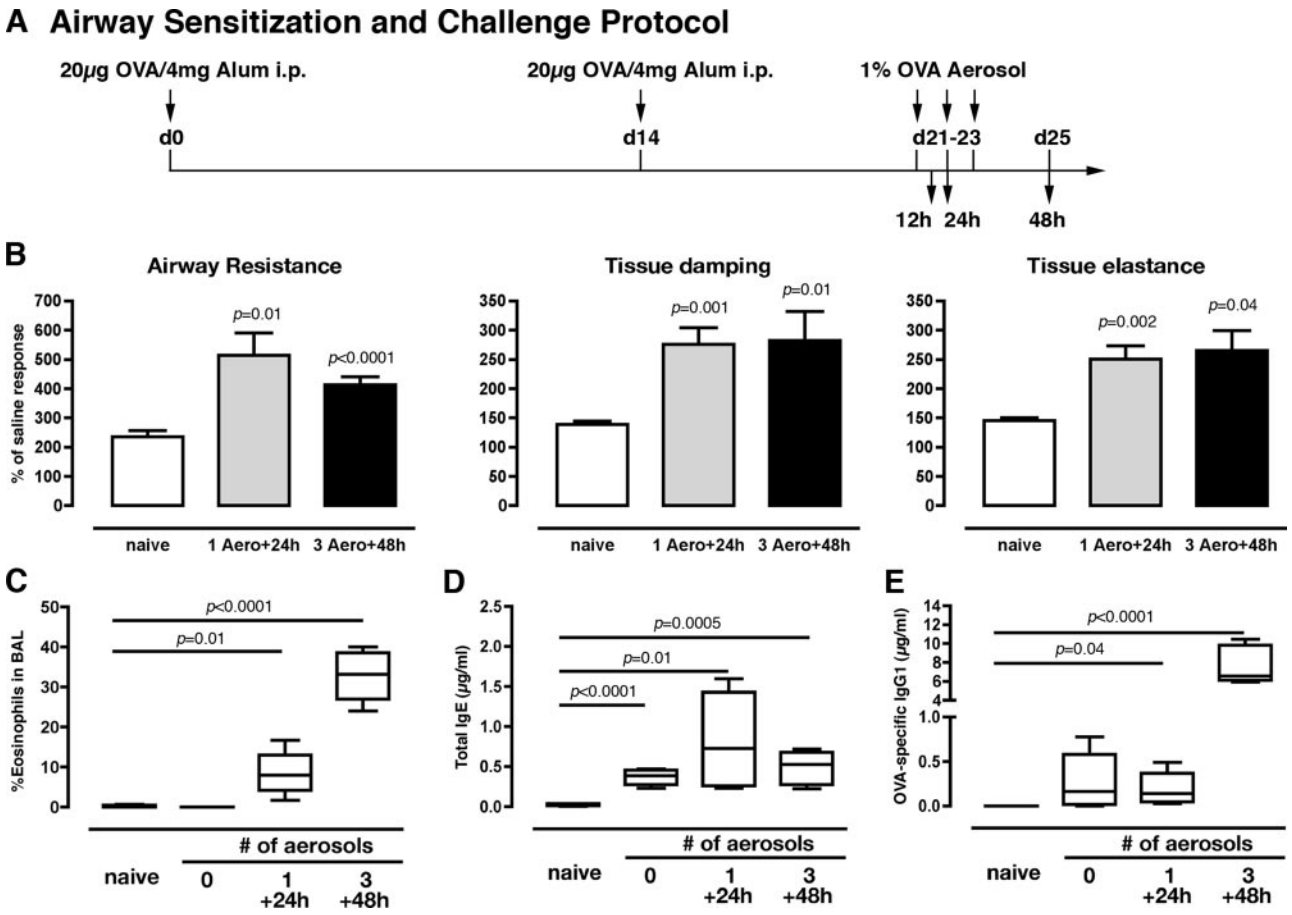

FIGURE 1. Characterization of the BALB/c mouse model of allergic airways inflammation. *A*, Sensitization protocol: animals were primed on days 0 and 14 and challenges were performed days 21–23. Serum was obtained in naive = nonsensitized controls; 1 Aero + 24 h = 24 h post 1 aerosol; 3 Aero + 48 h = 48 h post 3 aerosols. *B*, Lung functional changes during allergic airways sensitization measured by forced oscillometry after MCh challenge. Bar graphs represent mean ± SEM of 8 animals/group. Lung functional responses were expressed as a percentage of the response to the saline aerosol and compared using nonparametric ANOVA on ranks and Dunn's post-hoc test. Responses in tissue elastance were expressed as a percentage of the response to saline, $\log_{10}$ transformed, and compared using ANOVA and Tukey's post-hoc test. (*C*) BAL fluid eosinophilia, (*D*) serum total IgE, and (*E*) OVA-specific IgG1 levels following aerosol challenge at selected time points. BAL and serum were obtained from naive and preaerosol (0) mice and from mice at the indicated time points following OVA aerosol; mean values, upper and lower interquartiles, and spread of values for each group are displayed by the box and whisker plot using 5–10 animals/ group. Values of p were determined by Student's t test; n.s., nonsignificant.

mice that had received two doses of PBS in Alum i.p. (days 0 and 14) but were not exposed to OVA aerosols. Sera were pooled from at least 10 mice/group before 100–150 μl was administered i.v. to naive BALB/c mice. Each pool of sera was assayed for OVA-specific IgG1 and total IgE as described to confirm increased levels in the OVA-immune group and low levels in the control group.

Statistics

Parametric statistical analysis of data was performed with Prism software (GraphPad Software) using the unpaired, nonparametric Student t test unless otherwise indicated. Values of $p < 0.05$ were considered statistically significant. Lung functional responses in airway resistance and tissue damping to inhaled MCh at the maximum dose used (30 mg · ml^{-1}) were expressed as a percentage of the response to the saline aerosol and compared using nonparametric ANOVA on ranks and Dunn's post-hoc test. Responses in tissue elastance were expressed as a percentage of the response to saline, $\log_{10}$ transformed, and compared using ANOVA and Tukey's post-hoc test.

Results

Characterization of the BALB/c mouse model of EAAD

A BALB/c mouse model of OVA-induced EAAD was adopted to analyze RT-APC function during the onset of allergic airways inflammation. The sensitization protocol consisted of two systemic (i.p.) administrations of Alum-adsorbed OVA on days 0 and 14 (OVA sensitization), followed by exposure to aerosolized OVA (referred to as OVA challenge) at different time points (Fig. 1*A*). For the assessment of early changes, studies were conducted after 24 h following a single aerosol on day 21, while late and more chronic changes were investigated 48 h after the third of three daily aerosols administered on days 21–23. The primary clinical markers used to define EAAD are shown in Fig. 1, *B–E*. Lung functional changes were measured using forced oscillometry, a technique that enables partition of central airways resistance from peripheral lung parenchymal tissue damping and elastance. Twenty-four hours after a single aerosol challenge, significantly increased airways resistance, tissue damping, and tissue elastance were measured as compared with naive control mice (Fig. 1*B*). These parameters remained significantly elevated in the more chronic setting (48 h after three daily aerosols), although in the case of airways resistance, were starting to decline. The percentage of eosinophils was significantly increased in BAL fluid 24 h after a single OVA-aerosol exposure and continued to increase following multiple aerosols (Fig. 1*C*). In terms of Ab responses, total IgE

Downloaded from http://www.jimmunol.org/ by guest on October 27, 2021

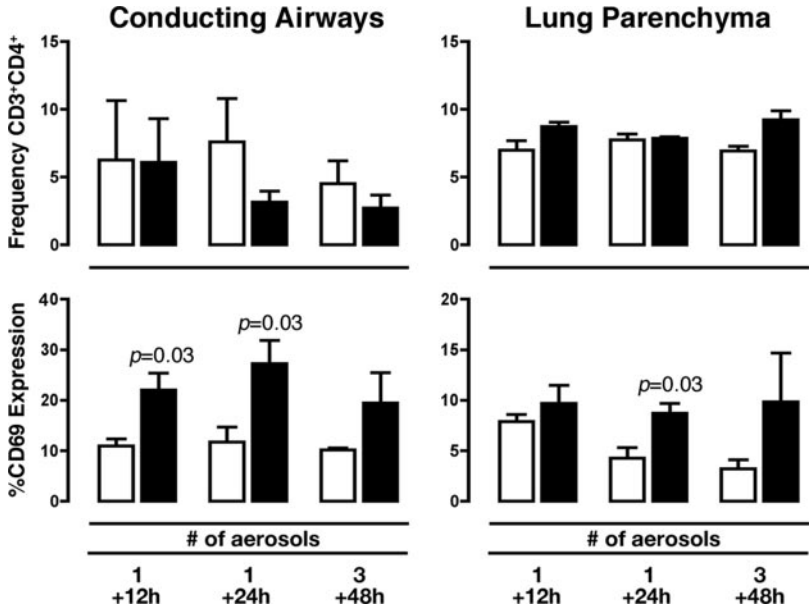

FIGURE 2. Kinetics of T cell activation during allergic airways sensitization. Cell suspensions were obtained from pooled tissue of 10 animals/group for conducting airways and lung parenchyma before analysis by flow cytometry as described in *Materials and Methods*. *Top panels* represent percentage frequency of $CD3^+CD4^+$ T cells and *bottom panels* represent percentage CD69 expression on $CD3^+CD4^+$ T cells from main conducting airways (*left panels*) and lung parenchyma (*right panels*). Bar graphs represent mean ± SEM of data from three to five experiments at the indicated time points: 1 Aero + 12 h = 12 h post 1 aerosol; 1 Aero + 24 h = 24 h post 1 aerosol; 3 Aero + 48 h = 48 h post 3 aerosols. Statistical analyses (*p*) comparing PBS controls (□) to OVA-sensitized animals (■) at the indicated time points following OVA-aerosol challenge were performed by Student's *t* test.

was measured (rather than OVA-specific IgE) due to the >14-fold higher OVA-specific IgG1 that were shown to interfere with measurement of OVA-specific IgE by ELISA in some groups (data not shown). Serum IgE levels showed an initial significant rise during the systemic sensitization phase before the first aerosol and remained elevated throughout the aerosol exposure period compared with control mice (Fig. 1*D*). OVA-specific IgG1 Ab production, in contrast, showed an early (but not significant) increase before aerosol exposure, and then further significant increases in response to single and multiple OVA-aerosol challenges ($p < 0.0001$ compared with the pre-aerosol and single-aerosol time point; Fig. 1*E*). In summary, the salient clinical features of the BALB/c mouse model of EAAD including increased airways resistance, BAL eosinophilia, and induction of serum IgE and IgG1 Abs resemble the hallmark clinical features of human allergic asthma.

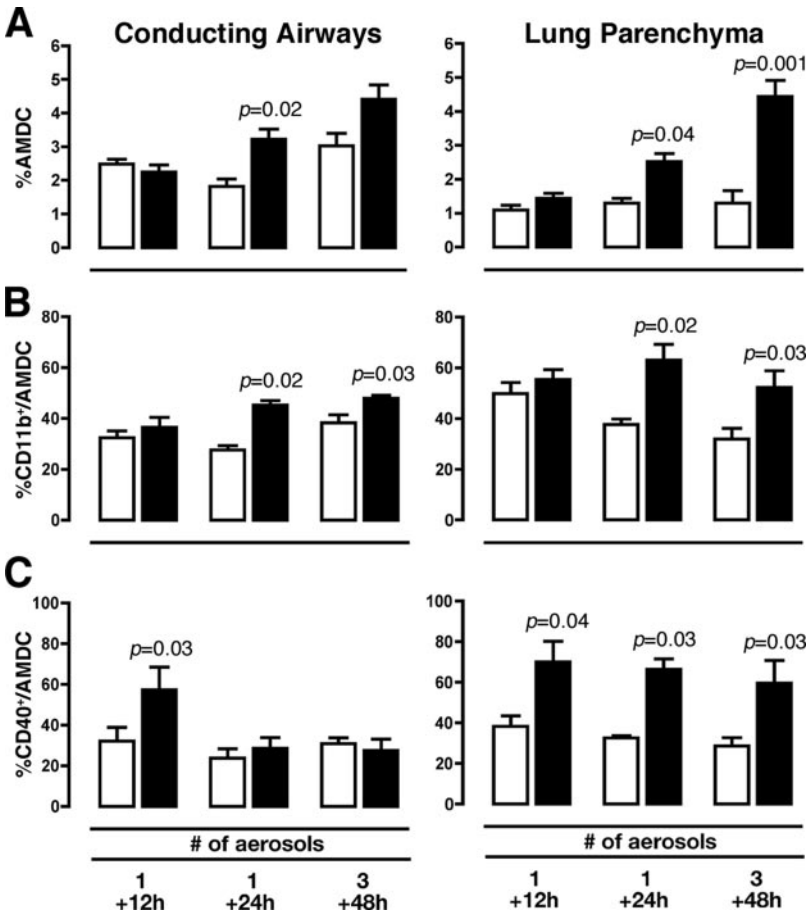

FIGURE 3. Kinetics and expression of CD11b and CD40 on $CD11c^+MHCII^+$ RT-DC during allergic airways sensitization. At the indicated time points after OVA-aerosol challenge, cell suspensions were obtained from pooled conducting airways and lung parenchyma tissue of 10 animals/group in PBS controls (□) and OVA-sensitized mice (■) before analysis by flow cytometry as described in *Materials and Methods*. (*A*) Kinetics of $CD11c^+MHCII^+$ airway DC, (*B*) percentage CD11b, and (*C*) percentage CD40 expression on $CD11c^+MHCII^+$ DC in main conducting airways (*left panels*) and lung parenchyma (*right panels*) after OVA-aerosol challenge. Bar graphs represent mean ± SEM of data from three to five experiments at the indicated time points: 1 Aero + 12 h = 12 h post 1 aerosol; 1 Aero + 24 h = 24 h post 1 aerosol; 3 Aero + 48 h = 48 h post 3 aerosols. Statistical analyses (*p*) comparing PBS controls (□) to OVA-sensitized animals (■) at the indicated time points following OVA-aerosol challenge were performed by Student's *t* test.

Downloaded from http://www.jimmunol.org/ by guest on October 27, 2021

Table I. *Summary of the phenotypic characteristics of mouse airway APC*

APC Type	I-A^d	CD11c	CD11b	CD2	CD16/32	CD54	CD103	CD115	CD205	F4/80	Gr1
B cell	+++[a]	−	−[b]	+++	+++	+++	−	−	+++	−	−
Macrophage	+++	+++[c]	+++	+++	+++	+++	+++[d]	−	+++	+++	++[e]
CD11b$^-$ DC	+++	+++	−[f]	−	+++	+++	+++[d]	−	+++	−	±[e]
CD11b$^+$ DC	+++	+++	+++	+	+++	+++	+++	−	+++	++	+[e]

[a] −, <10%; ±, 11–20%; + 21–40%; ++, 41–60%; +++, >61%.
[b] Approximately 10% of airway B cells are CD11b$^+$.
[c] Macrophages uniformly express low levels of CD11c compared to airway DC.
[d] Macrophages and CD11b$^+$ DC uniformly express intermediate levels of CD103 compared to CD11b$^-$ DC.
[e] Macrophages and DC expressed low or intermediate levels of Gr1 compared to granulocytes.
[f] CD11b$^-$ DC uniformly express low levels of CD11b compared to B cells.

CD4$^+$ T cell activation in anatomical compartments of the RT during aerosol allergen challenge

T cells are central in the pathogenesis of bronchial allergic asthma, with RT CD4$^+$ T cell activation considered to be a prerequisite event for the initiation of EAAD (12). Given the early physiological changes occurring in the conducting airways and lung parenchymal compartments described above, we examined whether any correlation existed between onset of functional changes and the kinetics of CD4$^+$ T cell activation within these compartments. Using the mouse model described above, we followed T cell activation kinetics in the RT during allergic airways sensitization, as measured by the expression of the early activation marker CD69 on CD3$^+$CD4$^+$ T cells. Frequencies of total (CD3$^+$CD4$^+$) and activated (CD3$^+$CD4$^+$CD69$^+$) T cells were determined in both tracheal tissue (referred to as conducting airways) and lung parenchyma at 12 and 24 h after a single aerosol challenge and 48 h after three aerosols. Although no significant changes were observed in the frequency of CD3$^+$CD4$^+$ T cells in either RT compartment (Fig. 2, *top panels*), a transient and significant increase in CD69 expression on CD4$^+$ T cells was observed in the conducting airways at 12 and 24 h after a single aerosol and at 24 h after a single aerosol in the lung parenchyma (Fig. 2, *bottom panels*). Thus, CD4$^+$ T cell activation occurred early following allergen challenge in the mucosa of the conducting airways (12–24 h), coinciding with the time point at which increased airways resistance was observed in this model (Fig. 1*B*).

Kinetics of RT-DC subset activation during onset of EAAD

The above data suggested that early activation of CD4$^+$ T cells in the mucosa of the conducting airways was a predisposing event for the development of airways hyperreactivity, a key clinical feature of EAAD and human allergic asthma. It is now well-established that RT-DC are important regulators of T cell activation in response to aeroallergen challenge, coordinating both T cell priming in DLN and local T cell activation within the RT (13). Therefore, we next sought to establish whether T cell activation within the RT was accompanied by changes in the frequency and/or activation status of RT-DC subsets in conducting airways and lung parenchyma. Single-cell suspensions prepared from the conducting airways and lung parenchyma were stained for CD11c and I/A-E (MHC class II (MHC II)) and RT-DC were identified as CD11c$^+$MHC II$^+$ by flow cytometry as previously described and shown in Fig. 5*A* (5). In the conducting airways, a transient but significant increase in the frequency of DC (hereafter referred to as AMDC; Fig. 3*A*, *left panel*), accompanied by an increase in the frequency of CD11b$^+$ AMDC (Fig. 3*B*, *left panel*), was observed 24 h after a single aerosol and to a lesser extent at 48 h after three aerosols. Increases were also observed in the lung parenchyma for total (Fig. 3*A*, *right panel*) and CD11b$^+$ RT-DC (Fig. 3*B*, *right panel*) at 24 h after a single aerosol, although much greater increases in DC frequency were observed at this site 48 h after three aerosols as compared with conducting airways (Fig. 3*A*, *right*

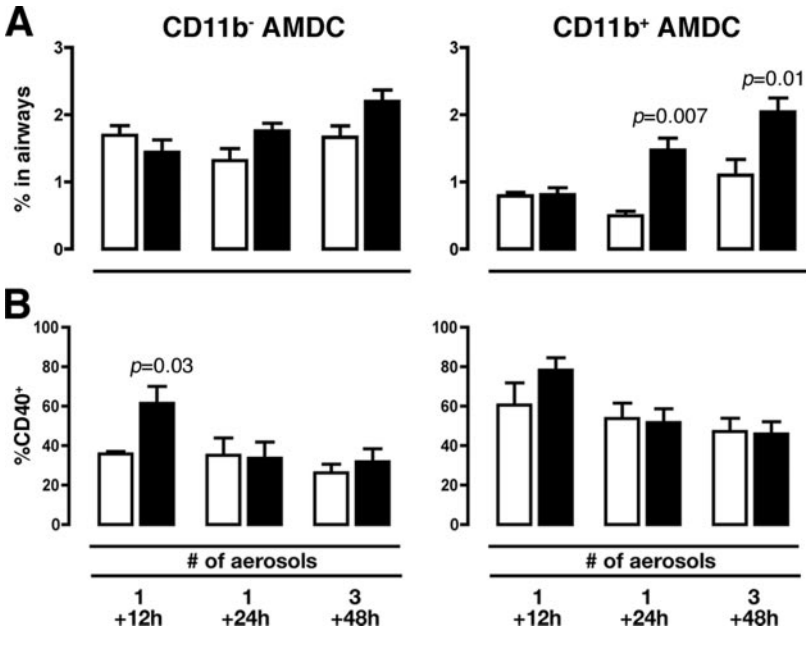

FIGURE 4. Subset kinetics and expression of CD40 on airway DC during allergic airways sensitization. At the indicated time points after OVA-aerosol challenge, cell suspensions were obtained from pooled conducting airways tissue of 10 animals/group in PBS controls (□) and OVA-sensitized mice (■) before analysis by flow cytometry as described in *Materials and Methods*. (*A*) Changes in frequency of CD11b$^+$ AMDC and CD11b$^-$ AMDC and (*B*) percentage CD40 expression during allergic airways sensitization. Bar graphs represent mean ± SEM of data from three to five experiments at the indicated time points: 1 Aero + 12 h = 12 h post 1 aerosol; 1 Aero + 24 h = 24 h post 1 aerosol; 3 Aero + 48 h = 48 h post 3 aerosols. Statistical analyses (*p*) comparing PBS controls (□) to OVA-sensitized animals (■) at the indicated time points following OVA-aerosol challenge were performed by Student's *t* test.

Downloaded from http://www.jimmunol.org/ by guest on October 27, 2021

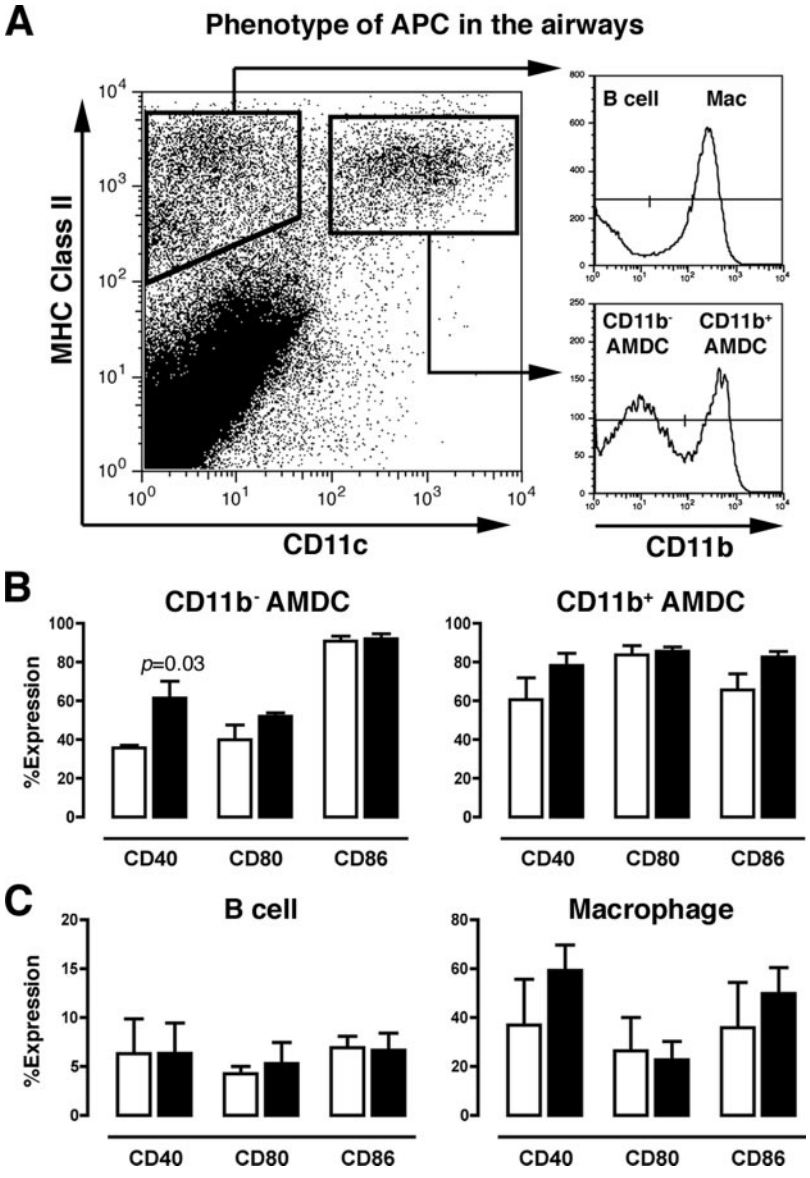

FIGURE 5. Costimulatory marker expression on airway APC during allergic airways sensitization. Twelve hours after OVA-aerosol challenge, cell suspensions were obtained from pooled conducting airways tissue of 10 animals per group in PBS controls (□) and OVA-sensitized mice (■) and analyzed by flow cytometry as described in *Materials and Methods*. *A*, Four APC populations (CD11b$^-$ AMDC, CD11b$^+$ AMDC, B cells, and macrophages) were identified in the airways on the basis of MHC class II, CD11c, and CD11b expression according to the gating strategy shown and as previously described (5). Frequency of CD40, CD80, and CD86 expression during allergic airways sensitization in (*B*) CD11b$^+$ AMDC and CD11b$^-$ AMDC and in (*C*) B cells and macrophages. Bar graphs represent mean ± SEM of data from three to five experiments. Statistical analyses (*p*) comparing PBS controls (□) to OVA-sensitized animals (■) at the indicated time points following OVA-aerosol challenge were performed by Student's *t* test.

panel). Interestingly, activation of RT-DC (as indicated by the frequency of cells expressing the costimulatory molecule CD40) was evident at the earliest time point examined in both anatomical compartments (Fig. 3*C*, *left* and *right panels*), preceding changes in RT-DC frequencies described above. However, CD40 expression peaked early and was short-lived in the main conducting airways (Fig. 3*C*, *left panel*), contrasting with the more sustained expression of this costimulatory molecule at the later time points in the lung parenchyma (Fig. 3*C*, *right panel*). These changes were restricted to up-regulation of CD40, as changes in other costimulatory molecules such as CD80 and CD86 were not observed in the airways at any of these time points (data not shown).

Within the conducting airways, the early transient activation of AMDC described above appeared to correlate with the early activation of CD4$^+$ T cells occurring in this anatomical site, prompting us to examine the kinetics of AMDC activation in more detail, especially subsets of these cells identified by the expression of CD11b (see Fig. 5*A*). We have found these two AMDC subsets differ in their expression of a number of other surface molecules, such as CD103 and F4/80 (Table I). In terms of subset frequencies, only the frequency of CD11b$^+$ AMDC was significantly increased 24 h after a single challenge and 48 h after three challenges (Fig. 4*A*). CD11b$^+$ AMDC, however, did not up-regulate CD40 expression at any time point (Fig. 4*B*, *right panel*), contrasting with the CD11b$^-$ AMDC subset which remained unchanged in terms of cell frequency (Fig. 4*A*, *left panel*) but displayed an early and transient up-regulation of CD40 expression 12 h following a single aerosol challenge (Fig. 4*B*, *left panel*). A summary of the main phenotypic characteristics of APC populations within murine conducting airways is provided in Table I.

To further investigate the effect of aerosol challenge on the activation status of AMDC, cells from the conducting airways were isolated 12 h after a single aerosol challenge (the time of peak CD4$^+$ T cell and AMDC activation in airways) and the expression of CD40, CD80, or CD86 was measured. At the same time, we also considered the expression of these molecules on two other APC populations, airway B cells, and macrophages, that can be identified by flow cytometry (Fig. 5*A*; see also Table I for a summary of phenotypic features). As previously observed, activation of AMDC was restricted to the CD11b$^-$ subset (Fig. 5*B*, *left panel*). Furthermore, AMDC activation was restricted to up-regulation of CD40 only, as no changes were observed in the expression of both CD80 and CD86 on both CD11b$^-$ and CDC11b$^+$ AMDC (Fig. 5*B*). Moreover, neither CD40, CD80, nor CD86 were

Downloaded from http://www.jimmunol.org/ by guest on October 27, 2021

up-regulated on airway B cells or macrophages, indicating that only the CD11b$^-$ subset of AMDC was involved (Fig. 5*C*). This was also the case for all other time points (data not shown). Thus, analysis of APC activation showed an early and transient up-regulation of CD40 expression that was restricted to CD11b$^-$ AMDC in the main conducting airways. Importantly, this activation coincided with an increase in the frequency of activated CD4$^+$ T cells in the airways.

Allergic airways sensitization leads to increased Ag-specific uptake and processing by airway APC

Because the kinetics of T cell activation and AMDC activation appeared to be closely related, we hypothesized that functional changes in AMDC, especially uptake and processing of Ag, may contribute to T cell activation within the conducting airways during the onset of EAAD. Thus, we sought to determine whether sensitization to OVA specifically increased OVA processing by AMDC, as assessed by the development of DQ-OVA fluorescence measured by flow cytometry, at the time of peak CD4$^+$ T cell and APC activation in airways (i.e., 12 h postchallenge). In this assay, DQ-OVA does not fluoresce until it is proteolytically cleaved into fragments, which we have previously shown correlates well with Ag processing for presentation by DC in the DLNs (9). In the present study, we collected the main conducting airways from sensitized mice 2 h after p.n. administration of a single DQ-OVA challenge (a time point previously determined to give an optimal in vivo DQ-OVA signal in DC), with an aim to measure Ag processing in situ before AMDC migration out of the tissue. AMDC were identified as above by labeling for CD11b, CD11c, and MHC class II and compared with a saline control to judge the extent of OVA processing (Fig. 6*A*). There were 2.9-fold more DQ-OVA$^+$ CD11b$^-$ AMDC and 3.6-fold more DQ-OVA$^+$CD11b$^+$ in the airways of OVA-sensitized mice as compared with PBS controls (Fig. 6*B*). We also observed an increase in DQ-OVA fluorescence in B cells (4.1-fold) and airway macrophages (3.2-fold), suggesting a general increase in processing by a variety of APC in the airways.

To confirm that the increase in DQ-OVA fluorescence was related to Ag capture by each APC population, we administered fluorescent conjugate of OVA (OVA-Alexa 647) p.n. and collected cells from the main conducting airways as described for DQ-OVA above. Compared with DQ-OVA, OVA-Alexa 647 does not require processing to fluoresce and is not affected by the acidic pH of Ag-processing compartment, so it can be detected intracellularly for at least 3 days after administration (data not shown). OVA was rapidly captured by cells in the airways of saline-sensitized mice, such that 15% of CD11b$^-$ AMDC, 54% of CD11b$^+$ AMDC, and 94% of airway macrophages were OVA$^+$ (Fig. 7*A*) 2 h after p.n. administration of OVA Alexa 647. In contrast, <1% of airway B cells were able to capture the OVA conjugate. Sensitization with OVA increased uptake by CD11b$^-$ AMDC 5.2-fold, CD11b$^+$ AMDC by 1.7-fold, and airway B cells by 52-fold, and while there was little change the proportion of OVA$^+$ macrophages, they were able to collect larger amounts of OVA as evidenced by an increase in mean fluorescence (Table II). Thus systemic Ag immunization improved Ag-specific uptake by all APC in the main conducting airways, correlating with the increase in DQ-OVA processing observed in the initial experiments.

We next tested the specificity of Ag capture by airway APC by using a second Ag, BLG from bovine milk, a protein which can also act as an allergen in the airways (14). Three groups of mice were sensitized, the first with PBS in Alum, the second with OVA in Alum, and the third with BLG in Alum. On day 21, all three groups were administered 50 μg of BLG-Alexa 647 in 50 μl of saline p.n. and the airways collected 2 h later. As before, a saline control was included to judge the amount of BLG uptake. We observed low levels of BLG uptake in CD11b$^-$ AMDC, CD11b$^+$ AMDC, and B cells from mice sensitized with PBS or OVA in Alum that were increased 12-, 3.7-, and 15-fold, respectively, in mice sensitized with BLG in Alum (Fig. 7*B*). There was little difference in the proportion of BLG$^+$ macrophages in each of the sensitized groups, but macrophages from BLG-sensitized mice were able to capture larger amounts of BLG than macrophages from PBS- or OVA-sensitized mice (Table II). All of the increases observed for BLG uptake in BLG-sensitized mice compared well with those seen for OVA uptake in OVA-sensitized mice (compare Fig. 7, *B* with *A*). Thus, allergic airways sensitization specifically increases the capacity of airway APC populations to capture the sensitizing Ag.

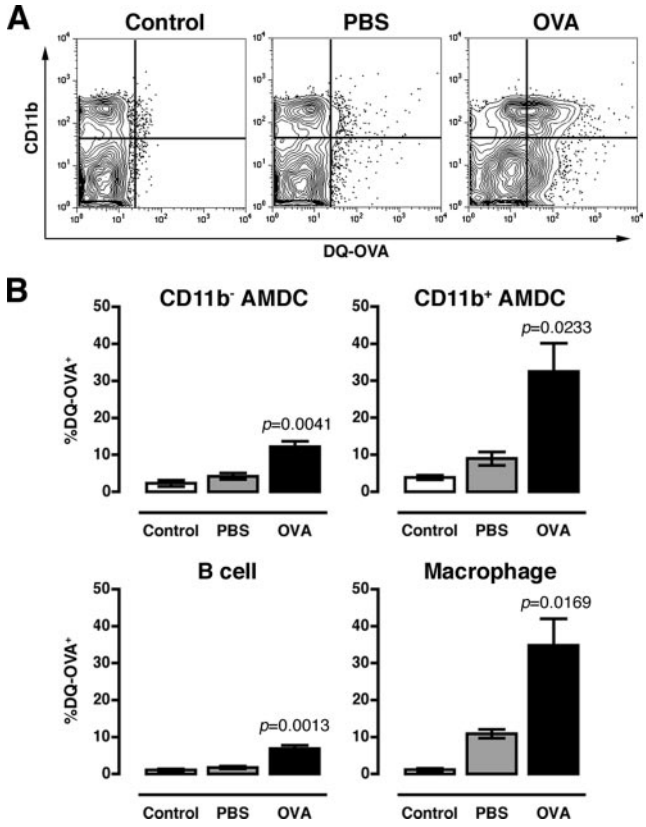

FIGURE 6. Sensitization increases Ag processing in airway APC populations. Two groups of five BALB/c mice were sensitized with PBS/Alum (PBS) or OVA/Alum (OVA) on days 0 and 14, then 40 μg of DQ-OVA was administered in 50 μl of saline p.n. on day 21. At the same time, a third group of OVA-sensitized mice (Control) were administered 50 μl of saline p.n. to serve as a control. The main conducting airways were collected 2 h later and prepared for flow cytometry. *A*, Representative plot showing DQ-OVA fluorescence in CD11b$^-$ and CD11b$^+$ AMDC from mice sensitized with PBS and OVA. *B*, DQ-OVA fluorescence was elevated in all airway APC populations from OVA-sensitized mice. Mean and SEM are shown for four independent experiments. Statistical analyses were performed comparing PBS controls (▨) to OVA-sensitized animals (■) using the Student's *t* test.

Passive immunization increases Ag uptake and processing in the airways

The allergen-specific increases in uptake and processing by airway APC observed in the above experiments suggested a role for Ag-specific Ig in facilitating allergen uptake and transport into airway

Downloaded from http://www.jimmunol.org/ by guest on October 27, 2021

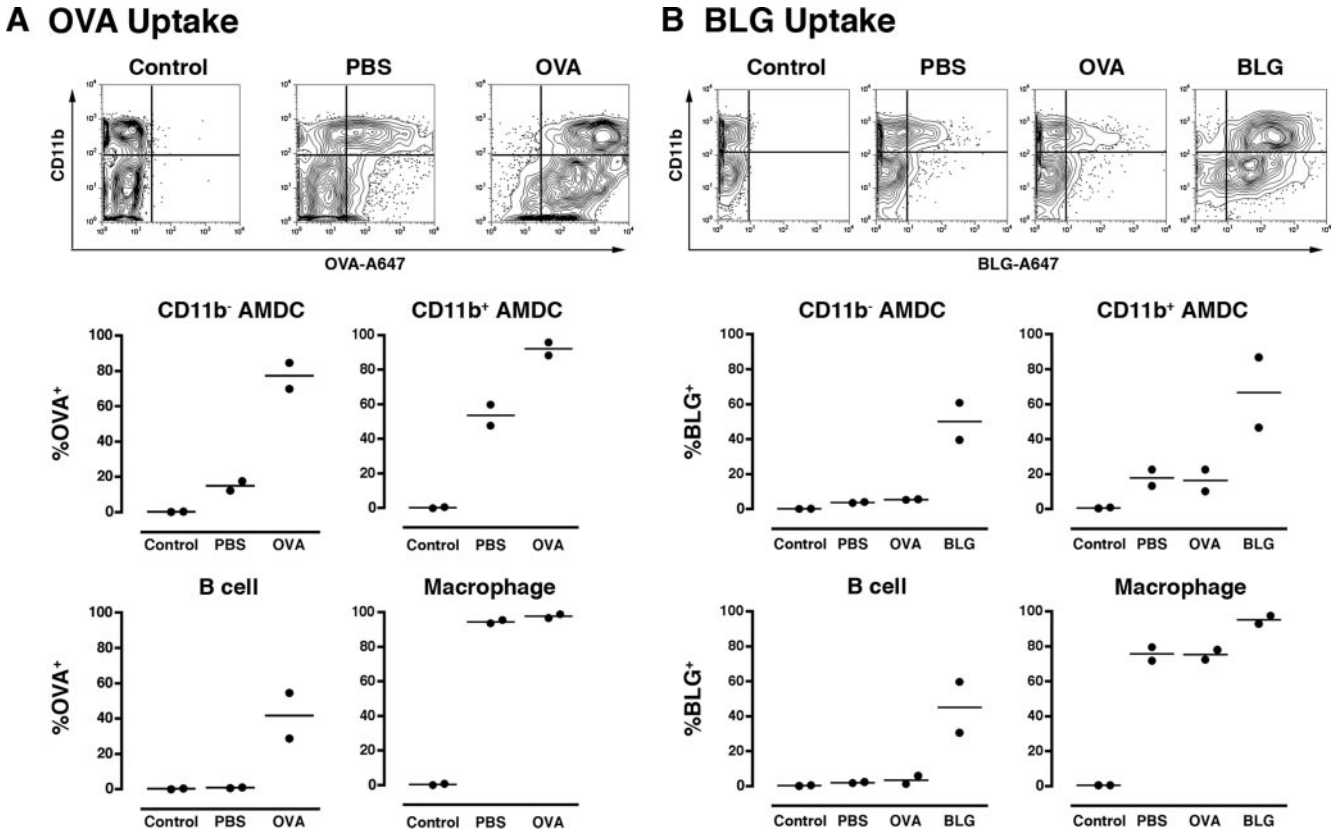

FIGURE 7. Immunization specifically increases Ag uptake by airway APC. *A*, Two groups of five BALB/c mice were sensitized with PBS/Alum (PBS) or OVA/Alum (OVA) on days 0 and 14, then 50 μg of OVA-A647 was administered in 50 μl of saline p.n. on day 21. The main conducting airways were collected 2 h later and Ag uptake was determined for CD11b$^-$ AMDC, CD11b$^+$ AMDC, B cells, and macrophages after comparison with a control group of OVA-sensitized mice administered 50 μl of saline p.n. (Control). *A*, Representative plots showing OVA-A647 uptake vs CD11b in total AMDC from each experimental group are shown in the *top panels. B*, Three groups of five BALB/c mice were sensitized with PBS/Alum (PBS), OVA/Alum (OVA), or BLG/Alum (BLG) before 50 μg of BLG-A647 was administered in 50 μl of saline p.n. on day 21. The main conducting airways were collected 2 h later and Ag uptake was determined for CD11b$^-$ AMDC, CD11b$^+$ AMDC, B cells, and macrophages after comparison with a control group of BLG -sensitized mice administered 50 μl of saline p.n. (Control). Representative plots showing BLG-A647 uptake vs CD11b in total AMDC from each experimental group are shown in the *top panels.* Results are shown for two independent experiments.

APC populations. To test this, we collected sera from OVA-sensitized and aerosol-challenged mice and used this to passively sensitize naive BALB/c mice by i.v. transfer. These sera contained high levels of OVA-specific IgG1, increased total IgE (Fig. 1*C*), and elevated levels of OVA-specific IgE as determined by capture ELISA (J. Burchell and P. A. Stumbles, data not shown). We also collected sera from mice sensitized with PBS in Alum (but were left unchallenged) to act as a control, because these contained low levels of IgE and undetectable levels of OVA-specific IgG1 (data not shown). Mice were administered 100–150 μl of sera i.v. and 24 h later, 20 μg of OVA-A647 plus 40 μg of DQ-OVA was administered p.n. The main conducting airways were isolated 2 h later and the amount OVA uptake and processing was determined for CD11b$^-$ AMDC, CD11b$^+$ AMDC, B cells, and macrophages with reference to a saline control (Fig. 8). Passive immunization with OVA-immune serum significantly increased OVA uptake by CD11b$^-$ AMDC, CD11b$^+$ AMDC, and B cells compared with mice administered control sera (Fig. 8, *A* and *B*). There was no difference in the proportion of airway macrophages that were OVA$^+$, but higher levels of OVA were seen in these cells in mice that had received OVA-immune sera as measured by the mean fluorescence for OVA-Alexa Fluor 647 (Table II). In contrast to OVA uptake, low levels of OVA processing were seen in B cells and CD11b$^-$ AMDC in both groups of sera recipients, while airway macrophages and CD11b$^+$ AMDC from mice passively immunized with OVA-immune sera contained significantly higher levels of DQ-OVA fluorescence than mice immunized with control sera (Fig. 8, *A* and *C*). To address the relative contribution of IgE and IgG in the current model, we heat-inactivated IgE by incubating sera at 56°C for 30 min (15, 16). Using this protocol, the absence of active IgE was confirmed, while OVA-specific IgG1 activity remained unchanged (data not shown). Passive immunization with heat-inactivated OVA-immune serum yielded identical results to native serum (data not shown), and therefore, suggested that the increase in OVA uptake and processing could be mediated by Ab isotypes other than IgE.

Passive immunization increases naive T cell activation in the airways after Ag exposure

In our previous studies on the primary response to inhaled Ag, we found that naive T cells were activated in the DLN within 12 h of administration, while activated T cells were not detected in the airways or lungs until day 3 (5, 9). These results contrast with the sensitized animals in the current study, where an increase in the proportion of CD4$^+$ T cells with an activated phenotype were observed in the main conducting airways as early as 12 h after one aerosol challenge (Fig. 2). We hypothesized that this early phase activation in the airways was a direct result of an increase in Ag presentation in situ. To test this hypothesis, we used DO11.10-transgenic mice that express an OVA-specific TCR on the majority of their CD4$^+$

Downloaded from http://www.jimmunol.org/ by guest on October 27, 2021

Table II. *OVA uptake by airway macrophages 2 h after p.n. administration*

		OVA Uptake		MFI	
		Expt. 1	Expt. 2	Expt. 1	Expt. 2
OVA uptake Alum sensitized:	PBS/Alum	95.4	93.5	1129	727
	OVA/Alum	98.9	96.7	1867	788
BLG uptake Alum sensitized:	PBS/Alum	71.9	79.6	46.9	141
	OVA/Alum	72.5	78.1	47.8	130
	BLG/Alum	93.0	97.5	224	620
OVA uptake passive immunization:	Control sera	88.1	40.6, 57.2	11,218	868, 1,909
	OVA sera	93.6	75.4, 72.9	14,497	5,117, 4,065

T cells. These mice offer the advantage that a population of OVA-specific naive $CD4^+$ T cells can readily be detected in the main conducting airways that are not normally present in wild-type animals. These cells are $CD44^{low}$ and $CD69^-$ compared with $CD44^{high}CD69^+$ memory cells that are found in the RT following infection or specific immunization (9, 17). DO11.10 mice were passively immunized with OVA immune or control sera as above, and then 100 μg of OVA was administered 24 h later. The main conducting airways and DLN were collected from each group at 16 h and the proportion of OVA-specific $CD4^+$ cells that were $CD44^{low}$ and $CD69^+$ (i.e., recently activated but otherwise naive) was determined by flow cytometry. The results were compared with a third group of unmanipulated DO11.10 to judge any increase in T cell activation. This third group of mice is an important control because our DO11.10 mice have not been bred on a RAG-deficient or SCID background to eliminate expression of endogenous TCR chains that allow dual reactivity with environmental Ags and promote memory T cell production (18, 19).

Approximately 2% of transgenic TCR^+, OVA-specific $CD4^+$ T cells were $CD44^{low}CD69^+$ in the DLN of unmanipulated DO11.10 mice, while up to 16% these cells in the airways were $CD44^{low}CD69^+$ (Fig. 9), presumably due to activation by environmental Ags (18, 19). After p.n. OVA immunization, an increase in T cell activation in the DLN of both groups of sera recipients was observed, but was significantly higher in mice passively sensitized with OVA-immune sera (Fig. 9, *left panel*). We also saw a significant increase in T cell activation in the airways of DO11.10 mice administered OVA-immune sera, whereas mice administered control sera resembled nonimmunized mice (Fig. 9, *right panel*). Thus, the increase in OVA uptake and processing mediated by passive immunization lead to an increase in OVA presentation.

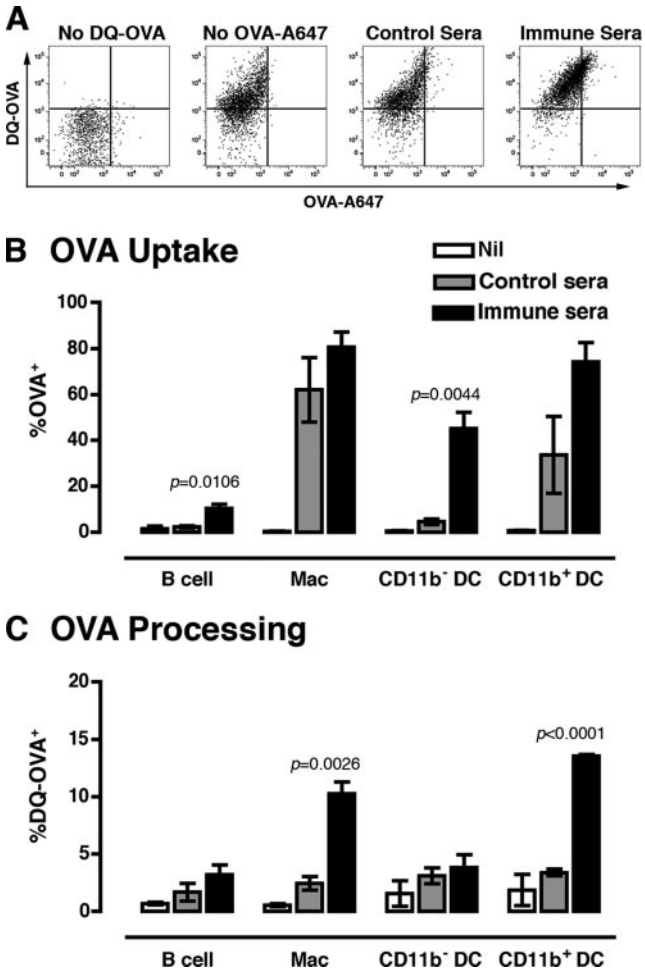

FIGURE 8. Passive immunization with immune sera increases Ag uptake and processing by airway APC. Two groups of 5–10 BALB/c mice were passively immunized with 100–150 μl of sera from PBS- or OVA-sensitized mice (Control sera, immune sera, respectively). Twenty-four hours later, 20 μg of OVA-A647 and 40 μg of DQ-OVA were administered in 50 μl of saline p.n. *A*, Representative plots showing OVA-A647 and DQ-OVA fluorescence for $CD11b^+$ AMDC from each group of sera recipients compared with naive mice administered 20 μg of OVA-A647 or 40 μg of DQ-OVA alone (no DQ-OVA, no OVA-A647, respectively). *B* and *C*, OVA uptake (*B*) and OVA processing (*C*), respectively, by $CD11b^-$ AMDC, $CD11b^+$ AMDC, B cells, and macrophages after comparison with a control group of naive mice administered 50 μl of saline p.n. (Nil). Mean and SEM are shown for three results from two independent experiments. Statistical analyses were performed comparing control sera (▨) to immune sera (■) using the Student's *t* test.

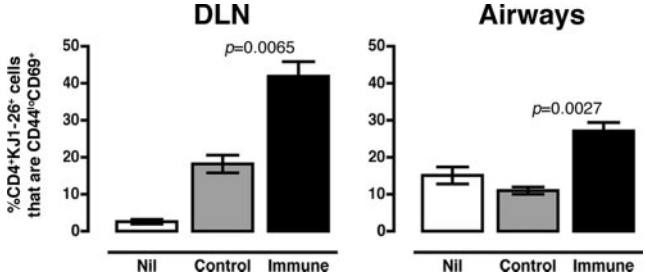

FIGURE 9. Passive immunization enhances T cell activation in the airways and DLN. Two groups of DO11.10 mice were passively immunized with 100–150 μl of sera from PBS- or OVA-sensitized mice (control sera, immune sera, respectively). Twenty-four hours later, each group was administered 100 μg of OVA in 50 μl of saline p.n. The airways and DLNs were collected 16 h later and the proportion of OVA-specific $CD4^+$ T cells that were $CD44^{low}CD69^+$ was determined by flow cytometry and compared with naive DO11.10 mice (Nil). Mean and SEM are shown for three independent experiments. Statistical analyses were performed comparing control sera (▨) to immune sera (■) using the Student's *t* test.

Downloaded from http://www.jimmunol.org/ by guest on October 27, 2021

Discussion

Allergic inflammatory airways diseases such as atopic bronchial asthma are a group of immunoinflammatory disorders of the central conducting airways and parenchymal lung tissue. Data from experimental mouse models indicate that the pathogenesis of these diseases is dependent on the actions of IL-4 and IL-5 and productive activation of Th2-biased $CD4^+$ T cells (20–24). Given the central role of $CD4^+$ T cell activation, recent attention has focused on professional APC such as RT-DC as key regulators of T cell activation during the induction of EAAD. Previous studies have demonstrated that induction of inflammation is dependent on DC and that myeloid DC derived from bone marrow or the RT have the capacity to prime Th2 responses to inhaled Ags (7, 25, 26). In addition, RT-DC have been shown to accelerate the translocation of antigenic signals to DLNs and to interact with $CD4^+$ T within the airway mucosa before the onset of disease (9, 12, 27, 28).

In the current study, we have extended these earlier studies to investigate in detail how RT-DC populations capture and process inhaled allergen within the RT during the early phases of EAAD onset. Our initial data showed that an early event occurring at the inception of the clinical symptoms following allergen challenge was the appearance of $CD69^+CD4^+$ T cells within the tissue of the conducting airways and lung parenchyma. These data are in agreement with recent studies showing a peak of 24 h for T cell recruitment into human airways following allergen challenge although mouse studies have shown a later peak for T cell recruitment into BAL fluid using a similar model of EAAD, perhaps reflecting a difference in the kinetics of T cell recruitment into tissue compartments as opposed to the airway lumen (29, 30). Nevertheless, these data are consistent with the conclusion that the early stages of allergic inflammation are an allergen-specific, $CD4^+$ T cell-mediated event.

The observed increased proportion of activated $CD4^+$ T cells within the airways after OVA challenge may be accounted for by several, nonmutually exclusive mechanisms. First, recently activated $CD4^+$ T cells may rapidly migrate from lymph nodes into the airways at the time of Ag exposure. On this point, we have detected activated T cells in draining and non-DLNs early after inhaled Ag delivery, which might be attributable to recirculation of activated cells from either the RT or from the DLN. However, we have failed to detect DC bearing inhaled Ag in the non-DLN at any stage, so it is likely these activated T cells are derived from known sites of Ag exposure (i.e., RT and DLN) (9).

Second, changes in the activation status of local APC populations may provide the necessary costimulatory signals to exceed the threshold requirements for local memory T cell activation within the airway mucosal tissue. On this basis, in the current study we analyzed the activation status of various APC populations within the RT, including AMDC subsets residing within the airway mucosa. The early appearance of activated $CD4^+$ T cells at this site coincided with an increase in the frequency of activated $CD11b^-$ AMDC expressing the CD40 (but not CD80 or CD86) costimulatory molecule. As previously reported, other rodent studies have identified changes in numbers and activation status of key APC populations such as AMDC during the onset of allergic airways disease and suggest that this process may be driven by local DC-$CD4^+$ T cell interactions occurring early after Ag inhalation (12, 25–27). Furthermore, our data suggest that $CD4^+$ T cell activation within conducting airways was, in part, driven by activation of $CD11b^-$ AMDC. The phenotype of $CD11b^-$ AMDC is compatible with that of a $CD103^+$ epithelial-derived DC previously described in the mouse lung and we have shown that $CD11b^-CD8a^{low}$ DC are one of the major Ag-bearing cell types in the DLN following p.n. exposure to OVA (6, 9). Although the underlying mechanism of $CD11b^-$ AMDC activation was not directly addressed in the current study, one hypothesis that this may in part be driven by interactions between allergen-bearing $CD11b^-$ AMDC and OVA-specific memory $CD4^+$ T cells within the airway epithelium. Alternatively, CD40 up-regulation may be mediated by interaction of OVA-Ig immune complexes with FcRs on DC, as previously demonstrated by Regnault et al. (31). To support this, we have preliminary data to show that CD40 is up-regulated on both $CD11b^-$ and $CD11b^+$ AMDC (but not airway B cells or macrophages) in an Ag-specific manner 12 h after p.n. delivery of OVA into mice that had been passively sensitized with OVA-immune serum (M. E. Wikstrom, unpublished data). CD40-CD40L interactions have been shown to be important in regulating DC migration into DLNs following cutaneous Ag delivery (32). An absence of CD40L signaling has been shown to inhibit the onset of allergic airways inflammation in gene knockout mice, and we have preliminary data to show that CD40L blockade during allergen sensitization interrupts the development of eosinophilia and Ig production in EAAD (Ref. 33 and P. A. Stumbles and L. Graca, unpublished data). Together, these data support the conclusion that CD40 expression by $CD11b^-$ AMDC may be an early checkpoint for T cell activation and initiation of airways inflammation in EAAD.

Third, allergic sensitization increased the capacity of all airway APC subsets analyzed, including $CD11b^+$ and $CD11b^-$ AMDC, B cells and airway interstitial macrophages, to capture and process inhaled Ag in an Ag-specific manner. The extent to which individual APC populations can contribute to local T cell activation within the RT is not clear; however, we have previously shown that B cells, but not macrophages, isolated from both lung parenchyma and main conducting airways efficiently present Ag and activate T cells in vitro suggesting that B cells may also be potential contributor to T cell activation within the airway mucosa (5). The Ag specificity of the up-regulated OVA uptake and processing by airway APC subsets in this model raised the possibility that elevated levels of allergen-specific IgG1 and/or IgE could play an opsonizing role by mediating enhanced allergen capture. This was confirmed by the observation that enhanced uptake of allergen by a range of airway APC subsets could be reproduced in naive mice by passive transfer of serum from OVA-immunized mice. In contrast to allergen uptake, however, enhanced allergen processing was not observed in $CD11b^-$ AMDC (which was the case in the active immunization model), suggesting that Ab alone cannot fully recapitulate the enhanced Ag handling in the airway mucosa observed after active induction of EAAD. Passive immune serum transfer also increased $CD4^+$ T cell activation in the airways and DLNs of DO11.10 TCR-transgenic mice, demonstrating that the increases in OVA uptake and processing detected early in the airways lead to an increase in Ag presentation and subsequent T cell activation. It will be important to determine whether any of the T cell activation we observed in the airways DO11.10 mice can be attributed to local Ag presentation and activation of recirculating naive T cells. Regardless, our data are consistent with previous studies indicating that both IgG1 and IgE are capable of mediating allergic airways inflammation and altered airways function (34).

A characteristic feature of the Ab response of the BALB/c model of EAAD was the production of high levels of both OVA-specific IgE as well as IgG1, raising the question of the relative contribution of each isotype to the observed changes in APC function following passive serum transfer. DC have been shown to express the high-affinity IgE receptor FcεRI on their surface that can capture IgE bound to allergen (35). Earlier studies have proposed a role for IgE in enhanced allergen uptake and processing

Downloaded from http://www.jimmunol.org/ by guest on October 27, 2021

and recently Kitamura et al. (37) have shown that the high-affinity IgG receptor FcγRI on APC populations was crucial during the sensitization phase for the development of allergic airway inflammation (36, 37). Although mice deficient for the FcRI common γ-chain (FcγRI$^{-/-}$) produced comparable IgE and IgG levels to wild-type mice, AHR and other inflammatory indicators were reduced in these animals; reconstitution of FcγRI$^{-/-}$ animals with wild-type bone marrow DC partially, and with spleen cells completely restored the allergic airways inflammation in this model (37). Furthermore, Oshiba et al. (34) have shown that passive transfer of anti-OVA IgE and IgG1, but not IgG2a and IgG3, resulted in increased airways reactivity and BAL fluid eosinophilia following OVA challenge.

We found that heat-inactivated serum retained the ability to mediate the observed functional changes in the airway APC populations observed with intact serum, indicating that at least in the context of the EAAD model, IgG1 is the dominant contributor to passive APC sensitization (data not shown). In some respects this is not surprising, as in our hands IgG1 is by far the predominant Ab isotype induced following OVA/Alum immunization and may be the principal APC-sensitizing agent in BALB/c mice. Nevertheless, other studies have shown Ag processing through FcεRI-mediated uptake is 1000 times more effective than allergen presented through other routes. Semper et al. (38) demonstrated increased surface expression of FcεRI on Langerhans cells in skin biopsies obtained from noninflamed sites in subjects with active atopic dermatitis, asthma, and allergic rhinitis. In allergic patients, FcεRI expression is up-regulated on DC and seemingly correlates with elevated IgE levels, while treating asthmatic individuals with anti-IgE reduced the exacerbation rate and reduced steroid requirements (39, 40). Others have also proposed a role for the low-affinity IgE receptor (FcεRII or CD23) in the pathogenesis of atopy and allergic airways disease in humans and mice (41–45). In humans, it has been proposed that a rate-limiting step may be the slow development and limited survival of IgE class-switched plasma cells and switching to IgG4 under periods of chronic, nonpathogenic allergen exposure (46). However, further studies with purified sources of IgE and IgG are required to determine the relative contribution of these Ab isotypes and their respective receptors to the up-regulation of airway APC function observed in the current model of EAAD.

In summary, previous studies have implicated transient up-regulation of the T cell-activating properties of local airway APC populations in the initiation of pathogenic CD4$^+$ T cell responses to inhaled Ag in EAAD, involving in particular increased costimulator expression by AMDC (12, 25, 27). The trigger for activation of these AMDC functions was shown to be provided via interaction with OVA-specific Th-memory cells. The present study provides supporting evidence for this hypothesis via the demonstration of CD40 up-regulation on AMDC, but importantly extends this concept to include parallel up-regulation of the Ag-uptake and -processing properties of AMDC. In our model, this process could be replicated by transfer of circulating Ag-specific IgG1 that acted to promote the retention and processing of immunogenic Ag within the airway mucosa. It is also possible that IgE may have contributed to this effect, however, we were unable to demonstrate this directly in these experiments. We have previously argued that the tight regulation of local Ag processing is critical in the maintenance of immunological homeostasis (8). The current data support a mechanism whereby high levels of circulating allergen-specific Ig can contribute toward the breakdown of local immunoregulation these in situ regulatory such that local Ag-processing and -presenting function is enhanced beyond the threshold required for local T cell activation. Current immunotherapeutic strategies for atopic asthma focus primarily on desensitization of allergen-specific CD4$^+$ Th cells. However, the present findings suggest that strategies targeting Ab-dependent, Ag-processing pathway through the combined approaches of neutralization of circulating IgG and IgE, B cell-targeted therapies and the functional blockade or modulation of FcR expression, also have potential for limiting the persistence of this disease.

Acknowledgment

We thank Laurent Nicod for critically reading the manuscript and for his helpful discussions.

Disclosures

The authors have no financial conflict of interest.

References

1. Sedgwick, J. D., and P. G. Holt. 1983. Induction of IgE-isotype specific tolerance by passive antigenic stimulation of the respiratory mucosa. *Immunology* 50: 625–630.
2. Tsitoura, D. C., R. H. DeKruyff, J. R. Lamb, and D. T. Umetsu. 1999. Intranasal exposure to protein antigen induces immunological tolerance mediated by functionally disabled CD4$^+$ T cells. *J. Immunol.* 163: 2592–2600.
3. Brimnes, M. K., L. Bonifaz, R. M. Steinman, and T. M. Moran. 2003. Influenza virus-induced dendritic cell maturation is associated with the induction of strong T cell immunity to a coadministered, normally nonimmunogenic protein. *J. Exp. Med.* 198: 133–144.
4. Lambrecht, B. N., and H. Hammad. 2003. Taking our breath away: dendritic cells in the pathogenesis of asthma. *Nat. Rev. Immunol.* 3: 994–1003.
5. von Garnier, C., L. Filgueira, M. Wikstrom, M. Smith, J. A. Thomas, D. H. Strickland, P. G. Holt, and P. A. Stumbles. 2005. Anatomical location determines the distribution and function of dendritic cells and other APCs in the respiratory tract. *J. Immunol.* 175: 1609–1618.
6. Sung, S. S., S. M. Fu, C. E. Rose, Jr., F. Gaskin, S. T. Ju, and S. R. Beaty. 2006. A major lung CD103 (α_E)-β_7 integrin-positive epithelial dendritic cell population expressing Langerin and tight junction proteins. *J. Immunol.* 176: 2161–2172.
7. Stumbles, P. A., J. A. Thomas, C. L. Pimm, P. T. Lee, T. J. Venaille, S. Proksch, and P. G. Holt. 1998. Resting respiratory tract dendritic cells preferentially stimulate T helper cell type 2 (Th2) responses and require obligatory cytokine signals for induction of Th1 immunity. *J. Exp. Med.* 188: 2019–2031.
8. Holt, P. G., and P. A. Stumbles. 2000. Regulation of immunologic homeostasis in peripheral tissues by dendritic cells: the respiratory tract as a paradigm. *J. Allergy Clin. Immunol.* 105: 421–429.
9. Wikstrom, M. E., E. Batanero, M. Smith, J. A. Thomas, C. von Garnier, P. G. Holt, and P. A. Stumbles. 2006. Influence of mucosal adjuvants on antigen passage and CD4$^+$ T cell activation during the primary response to airborne allergen. *J. Immunol.* 177: 913–924.
10. Hantos, Z., R. A. Collins, D. J. Turner, T. Z. Janosi, and P. D. Sly. 2003. Tracking of airway and tissue mechanics during TLC maneuvers in mice. *J. Appl. Physiol.* 95: 1695–1705.
11. Hantos, Z., A. Adamicza, E. Govaerts, and B. Daroczy. 1992. Mechanical impedances of lungs and chest wall in the cat. *J. Appl. Physiol.* 73: 427–433.
12. Huh, J. C., D. H. Strickland, F. L. Jahnsen, D. J. Turner, J. A. Thomas, S. Napoli, I. Tobagus, P. A. Stumbles, P. D. Sly, and P. G. Holt. 2003. Bidirectional interactions between antigen-bearing respiratory tract dendritic cells (DCs) and T cells precede the late phase reaction in experimental asthma: DC activation occurs in the airway mucosa but not in the lung parenchyma. *J. Exp. Med.* 198: 19–30.
13. Stumbles, P. A., J. W. Upham, and P. G. Holt. 2003. Airway dendritic cells: co-ordinators of immunological homeostasis and immunity in the respiratory tract. *Apmis* 111: 741–755.
14. Adel-Patient, K., M. A. Nahori, B. Proust, J. R. Lapa e Silva, C. Creminon, J. M. Wal, and B. B. Vargaftig. 2003. Elicitation of the allergic reaction in β-lactoglobulin-sensitized BALB/c mice: biochemical and clinical manifestations differ according to the structure of the allergen used for challenge. *Clin. Exp. Allergy* 33: 376–385.
15. Ishizaka, K., T. Ishizaka, and A. E. Menzel. 1967. Physicochemical properties of reaginic antibody. VI. Effect of heat on γ-E-, γ-G- and γ-A-antibodies in the sera of ragweed sensitive patients. *J. Immunol.* 99: 610–618.
16. Dorrington, K. J., and H. Bennich. 1973. Thermally induced structural changes in immunoglobulin E. *J. Biol. Chem.* 248: 8378–8384.
17. Woodland, D. L., K. H. Ely, S. R. Crowe, M. Tighe, J. W. Brennan, A. G. Harmsen, and L. S. Cauley. 2002. Antiviral memory T-cell responses in the lung. *Microbes Infect.* 4: 1091–1098.
18. Lee, W. T., J. Cole-Calkins, and N. E. Street. 1996. Memory T cell development in the absence of specific antigen priming. *J. Immunol.* 157: 5300–5307.
19. Hurst, S. D., S. M. Sitterding, S. Ji, and T. A. Barrett. 1997. Functional differentiation of T cells in the intestine of T cell receptor transgenic mice. *Proc. Natl. Acad. Sci. USA* 94: 3920–3925.
20. Hogan, S. P., A. Mould, H. Kikutani, A. J. Ramsay, and P. S. Foster. 1997. Aeroallergen-induced eosinophilic inflammation, lung damage, and airways hyperreactivity in mice can occur independently of IL-4 and allergen-specific immunoglobulins. *J. Clin. Invest.* 99: 1329–1339.

Downloaded from http://www.jimmunol.org/ by guest on October 27, 2021

21. Kuperman, D., B. Schofield, M. Wills-Karp, and M. J. Grusby. 1998. Signal transducer and activator of transcription factor 6 (Stat6)-deficient mice are protected from antigen-induced airway hyperresponsiveness and mucus production. *J. Exp. Med.* 187: 939–948.
22. Jember, A. G.-H., R. Zuberi, F.-T. Liu, and M. Croft. 2001. Development of allergic inflammation in a murine model of asthma is dependent on the costimulatory receptor OX40. *J. Exp. Med.* 193: 387–392.
23. Li, L., M. Crowley, A. Nguyen, and D. Lo. 1999. Ability of a non-depleting anti-CD4 antibody to inhibit Th2 responses and allergic lung inflammation is independent of coreceptor function. *J. Immunol.* 163: 6557–6566.
24. Mueller, C., and A. August. 2003. Attenuation of immunological symptoms of allergic asthma in mice lacking the tyrosine kinase ITK. *J. Immunol.* 170: 5056–5063.
25. Lambrecht, B. N., B. Salomon, D. Klatzmann, and R. A. Pauwels. 1998. Dendritic cells are required for the development of chronic eosinophilic airway inflammation in response to inhaled antigen in sensitized mice. *J. Immunol.* 160: 4090–4097.
26. Lambrecht, B. N., M. De Veerman, A. J. Coyle, J.-C. Gutierrez-Ramos, K. Thielemans, and R. A. Pauwels. 2000. Myeloid dendritic cells induce Th2 responses to inhaled antigen, leading to eosinophilic airway inflammation. *J. Clin. Invest.* 106: 551–559.
27. Vermaelen, K., and R. Pauwels. 2003. Accelerated airway dendritic cell maturation, trafficking, and elimination in a mouse model of asthma. *Am. J. Respir. Cell. Mol. Biol.* 29: 405–409.
28. Vermaelen, K. Y., I. Carro-Muino, B. N. Lambrecht, and R. A. Pauwels. 2001. Specific migratory dendritic cells rapidly transport antigen from the airways to the thoracic lymph nodes. *J. Exp. Med.* 193: 51–60.
29. Kariyawasam, H. H., M. Aizen, J. Barkans, D. S. Robinson, and A. B. Kay. 2007. Remodelling and AHR but not cellular inflammation persist after allergen challenge in asthma. *Am. J. Respir. Crit. Care Med.* 175: 896–904.
30. Lommatzsch, M., P. Julius, M. Kuepper, H. Garn, K. Bratke, S. Irmscher, W. Luttmann, H. Renz, A. Braun, and J. C. Virchow. 2006. The course of allergen-induced leukocyte infiltration in human and experimental asthma. *J. Allergy Clin. Immunol.* 118: 91–97.
31. Regnault, A., D. Lankar, V. Lacabanne, A. Rodriguez, C. Thery, M. Rescigno, T. Saito, S. Verbeek, C. Bonnerot, P. Ricciardi-Castagnoli, and S. Amigorena. 1999. Fcγ receptor-mediated induction of dendritic cell maturation and major histocompatibility complex class I-restricted antigen presentation after immune complex internalization. *J. Exp. Med.* 189: 371–380.
32. Moodycliffe, A. M., V. Shreedhar, S. E. Ullrich, J. Walterscheid, C. Bucana, M. L. Kripke, and L. Flores-Romo. 2000. CD40-CD40 ligand interactions in vivo regulate migration of antigen-bearing dendritic cells from the skin to draining lymph nodes. *J. Exp. Med.* 191: 2011–2020.
33. Lei, X. F., Y. Ohkawara, M. R. Stampfli, C. Mastruzzo, R. A. Marr, D. Snider, Z. Xing, and M. Jordana. 1998. Disruption of antigen-induced inflammatory responses in CD40 ligand knockout mice. *J. Clin. Invest.* 101: 1342–1353.
34. Oshiba, A., E. Hamelmann, K. Takeda, K. L. Bradley, J. E. Loader, G. L. Larsen, and E. W. Gelfand. 1996. Passive transfer of immediate hypersensitivity and airway hyperresponsiveness by allergen-specific immunoglobulin (Ig) E and IgG1 in mice. *J. Clin. Invest.* 97: 1398–1408.
35. Maurer, D., E. Fiebiger, B. Reininger, C. Ebner, P. Petzelbauer, G. P. Shi, H. A. Chapman, and G. Stingl. 1998. Fcε receptor I on dendritic cells delivers IgE-bound multivalent antigens into a cathepsin S-dependent pathway of MHC class II presentation. *J. Immunol.* 161: 2731–2739.
36. Mudde, G. C., R. Bheekha, and C. A. F. M. Bruijnzeel-Koomen. 1995. Consequences of IgE/CD23-mediated antigen presentation in allergy. *Immunol. Today* 16: 380–383.
37. Kitamura, K., K. Takeda, T. Koya, N. Miyahara, T. Kodama, A. Dakhama, T. Takai, A. Hirano, M. Tanimoto, M. Harada, and E. W. Gelfand. 2007. Critical role of the Fc receptor γ-chain on APCs in the development of allergen-induced airway hyperresponsiveness and inflammation. *J. Immunol.* 178: 480–488.
38. Semper, A. E., K. Heron, A. C. Woollard, J. P. Kochan, P. S. Friedmann, M. K. Church, and I. G. Reischl. 2003. Surface expression of FcεRI on Langerhans' cells of clinically uninvolved skin is associated with disease activity in atopic dermatitis, allergic asthma, and rhinitis. *J. Allergy Clin. Immunol.* 112: 411–419.
39. Foster, B., D. D. Metcalfe, and C. Prussin. 2003. Human dendritic cell 1 and dendritic cell 2 subsets express FcεRI: correlation with serum IgE and allergic asthma. *J. Allergy Clin. Immunol.* 112: 1132–1138.
40. Soler, M., J. Matz, R. Townley, R. Buhl, J. O'Brien, H. Fox, J. Thirlwell, N. Gupta, and G. Della Cioppa. 2001. The anti-IgE antibody omalizumab reduces exacerbations and steroid requirement in allergic asthmatics. *Eur. Respir. J.* 18: 254–261.
41. Delespesse, G., U. Suter, D. Mossalayi, B. Bettler, M. Sarfati, H. Hofstetter, E. Kilcherr, P. Debre, and A. Dalloul. 1991. Expression, structure, and function of the CD23 antigen. *Adv. Immunol.* 49: 149–191.
42. Haczku, A., K. Takeda, E. Hamelmann, A. Oshiba, J. Loader, A. Joetham, C. Irvin, H. Kikutani, and E. W. Gelfand. 1997. CD23 deficient mice develop allergic airway hyperresponsiveness following sensitization with ovalbumin. *Am. J. Respir. Crit. Care Med.* 156: 1945–1955.
43. Hakonarson, H., C. Carter, C. Kim, and M. M. Grunstein. 1999. Altered expression and action of the low-affinity IgE receptor FcεRII (CD23) in asthmatic airway smooth muscle. *J. Allergy Clin. Immunol.* 104: 575–584.
44. Riffo-Vasquez, Y., D. Spina, M. Thomas, T. Gilbey, D. M. Kemeny, and C. P. Page. 2000. The role of CD23 on allergen-induced IgE levels, pulmonary eosinophilia and bronchial hyperresponsiveness in mice. *Clin. Exp. Allergy* 30: 728–738.
45. Rosenwasser, L. J., W. W. Busse, R. G. Lizambri, T. A. Olejnik, and M. C. Totoritis. 2003. Allergic asthma and an anti-CD23 mAb (IDEC-152): results of a phase I, single-dose, dose-escalating clinical trial. *J. Allergy Clin. Immunol.* 112: 563–570.
46. Aalberse, R. C., and T. A. E. Platts-Mills. 2004. How do we avoid developing allergy: modifications of the TH2 response from a B-cell perspective. *J. Allergy Clin. Immunol.* 113: 983–986.

Downloaded from http://www.jimmunol.org/ by guest on October 27, 2021